3-4-3 Long-term Data Analysis of Ionosphere over Syowa Station, Antarctica

MOTOBA Tetsuo

The Earth's ionosphere is a partially ionized gas (electrons and ions) that forms several regions between the atmosphere and space over about 70 km height. The ionosonde is one of the radar techniques to monitor the ionospheric electron density as a function of height. The ionosonde transmits HF radio wave (1–30 MHz) vertically and receives echoes reflected from the various ionized layers. The F2-layer critical frequency (foF2), which is a principal parameter obtained from the ionosondes, corresponds to F2-layer peak electron density. In this study, we present ionospheric F2-layer variability (in particular, solar/geomagnetic activity dependence of the local time and seasonal behavior, and a long-term trend) over Syowa Station (69.0° S, 39.6° E), Antarctica, on the basis of long-term ionospheric database in 1959–2002.

Keywords
Ionospheric variability, Ionosonde, foF2, Syowa Station

1 Introduction

In the Earth's upper atmosphere at an altitude higher than 60 km, there is a region with significant electrical conductivity. The ionized region (called the Ionosphere) is mainly produced by extreme solar ultraviolet (EUV, 10~120 nm wavelength) radiation and X-rays that ionize the neutral atmosphere. The ionosphere is classified into several regions according to the electron density profile. The ionospheric region at an altitude ranging from 90 to 130 km is called the E region, and that ranging from 130 to 1000 km is known as the F region. During the daytime, the D region appears below the E region (at altitudes of 60 to 90 km), while the F region is divided into the F1 region (at altitudes of 130 to 210 km) and F2 region (at altitudes of 210 to 1,000 km) during the daytime except in winter. The basic plasma structure in the ionosphere is determined by the balance in the production process due to solar radiation (particularly EUV and X-rays), the loss process due to the photochemical process, the recombination process of ions and electrons, the transport process due to gravity, diffusion and electromagnetic effects, and other factors. On the other hand, electron density in the ionosphere is up to 0.1% lower than neutral density in the upper atmosphere. In other words, the ionosphere can be called a "weakly ionized plasma region." Therefore, the neutral dynamics plays an important role in ionospheric variations. In addition, as the ionosphere is also affected by strong coupling processes (such as solar and geomagnetic activity) in the regions above and below (such as tidal waves, gravity waves, and planetary waves), temporal, regional and seasonal variations of the ionosphere are more complicated.

Ionospheric observation using ionosondes has a long history. Ionosonde observation is useful worldwide as a means of monitoring ionospheric electron density[1]. The ionosonde (or ionospheric sounder) is a kind of radar that transmits high frequency (HF: 1~30 MHz) radio signals while sweeping those frequen-

cies, and receives the signals reflected from the ionosphere. The ionosonde allows the reflection height of radio waves to be determined based on the time delay in signals. However, since the group velocity of radio waves is slowed by any ionization, determining the reflection height based on the time delay is not so simple. For example, if radio waves with frequency f encounter another layer whose plasma frequency is higher than the frequency of the wave, it will be reflected with the return signal being further delayed as it travels back through the underlying ionization. The apparent/virtual height h'(f) indicated by this time delay will therefore be higher than the true reflection altitude h(f). Moreover, two independent types of radio waves are transmitted: one is the left-hand ordinary polarized mode whose reflection is determined by local electron density, whereas the other is the right-hand extraordinary polarized mode whose reflection is also affected by the local magnetic field. The first type is known as O-mode (ordinary mode), while the second is known as X-mode (extraordinary mode). The ionosonde uses a linearly polarized wave represented by two circularly polarized waves rotating in opposite senses.

The ionosonde on the ground can obtain electron density profiles lower than the altitude of maximum electronic density in the ionosphere (at 200 to 400 km), by transmitting signals sweeping in frequency from 1 to 30 MHz and recording the time delay it takes the signal to be reflected back to the receiver. The maximum frequency (critical frequency) of signals reflected in the ionosphere corresponds to the maximum electron density, and signals with even higher frequencies pass through the ionosphere. Ionograms are images of frequency f versus the time delay (virtual height h'(f)) of HF echoes from the ionosphere as recorded by an ionosonde. From an ionogram, one can directly determine the critical frequency of the F2 layer (foF2) corresponding to ordinary mode and the minimum virtual height (h'F2). During the daytime, the critical frequencies of the F1 layer and E layer, and the minimum virtual heights can be determined. Note that foF2 can be expressed by the maximum ionospheric electron density of the F2 layer (NmF2), where NmF2 (m^{-3}) $\approx 1.24 \times 10^{10} \times$ [foF2 (MHz)]^2.

Since the International Geophysical Year (IGY) in 1957 to 1958, steady ionospheric observation with an ionosonde has been conducted at Syowa Station in Antarctica. During about half a century up to the present, ionosonde data have been almost continuously accumulated, and play an important role in monitoring long-term changes in the Antarctic ionosphere. This paper describes ionospheric F2-layer variability in the auroral zone based on long-term ionosonde foF2 data obtained from 1959 to 2002 at Syowa Station, Antarctica (69.0° S, 39.6° E). In particular, the effects of solar and geomagnetic activity on seasonal and local time variations in the F2-layer electron density at Syowa, and the long-term trends over several decades are presented. The phenomenon of "global warming" of the earth's surface has recently been considered a major social issue, as it may lead to various global-scale environmental changes and subsequent destruction. This paper also discusses whether there are any indirect effects on the ionosphere over Syowa Station, based on long-term trend analysis.

2 Ionospheric variability over Syowa Station, Antarctica

2.1 Dependence on solar activity in foF2 relation with the solar activity cycle

This section first describes the long-term ionosonde dataset observed at Syowa Station. Ionospheric parameters (such as foF2) at each layer can be obtained based on an ionogram's graphical presentation of echo virtual height vs. sounding frequency every 15 minutes. Figure 1 shows the rate (%) of samples of the 1-h foF2 data taken at Syowa Station for each year from 1959 to 2002. The rate of 100% means that foF2 data were continuously obtained for one year (365 days). At Syowa

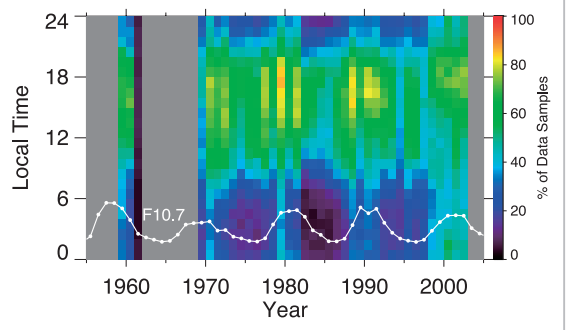

Fig.1 *Distribution of annual data acquisition rate (%) of foF2 data as a function of year and local time at Syowa Station from 1959 to 2002*

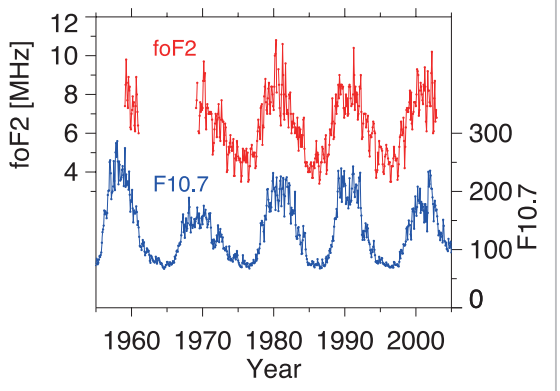

Fig.2 *Monthly median values of foF2 for hours around local noon (1100 to 1300 LT) at Syowa Station as presented together with monthly mean F10.7 values*

Station in this figure, it is necessary to note that there is an unfortunate data gap from 1962 to 1968, probably due to suspended ionosonde observation. The data acquisition rate is higher through all local times after 1997 because of an instrumental change from old analog system recording (film recording) to new digital system recording. As shown in this figure, the data acquisition status of foF2 changes significantly according to the local time each year. Data acquisition tends to be stable (at 60% or more) in the pre-noon to post-evening sector (about 1000 LT to 2000 LT), while it tends to decrease in the pre-midnight to morning sector (about 2200 LT to 0600 LT). In the post-midnight sector, the acquisition rate often drops below 20%. The lower data acquisition rate in the nighttime sector is presumably due to the depletion of F-layer electron density below the ionosonde's detection limit or an extreme enhancement in electron density in the lower ionosphere (particularly the D region) caused by the precipitation of higher energy particles (10 keV or more) during auroral activity. The enhanced electron density in the lower ionosphere causes the absorption of HF radio waves in what is called a "blackout." Moreover, the absorption of HF radio waves is also caused by auroral sporadic E (auroral Es). The diffusion of radio waves that are supposed to reach the F layer due to an abnormal ionospheric phenomenon near the E layer that appears along with auroral activity in the polar region during nighttime or auroral sporadic E (auroral Es), is another important factor that often inhibits F layer observation. The bottom of Fig. 1 shows long-term changes in the annual average of F10.7 solar radio wave flux (white line). F10.7 is a measure of solar radio flux [1 solar flux unit (SFU) = 10^{-22} Wm^{-2} Hz^{-1}] with a wavelength of 10.7 cm (2.8 GHz), and a proxy of changes in solar EUV radiation. The F10.7 is high for the solar maximum, while low for the solar minimum. When comparing F10.7 with the foF2 data acquisition rate at Syowa Station, we can see that the foF2 data acquisition rate tends to be higher for the solar maximum than the solar minimum. During the solar maximum, since the whole ionospheric altitude increases, ionosonde observation of the F region is effective. In contrast, since the ionospheric altitude decreases during the solar minimum, ionosonde observation is difficult, especially at nighttime. Therefore, the data acquisition rate is considered to be lower during the solar minimum.

Figure 2 shows the monthly median foF2 data at around local noon (1100 to 1300 LT) from Syowa Station, Antarctica, together with the monthly mean F10.7 data (blue line). In this figure, note that the foF2 variation is strongly influenced by solar activity with about an 11-year cycle from the solar maximum to solar minimum. This result shows that

the F-region electron density increases (decreases) with increasing (decreasing) solar EUV radiation during the solar maximum (minimum).

Figure 3 shows a scatter plot of the monthly median foF2 values versus the monthly mean F10.7 values. The red line shows a linear regression line of Y = aX + b (a = 0.026, b = 2.931), with a correlation coefficient of 0.896. The blue circles represent the mean foF2 values, averaging foF2 as divided by F10.7 for every 15 SFU. Error bars on the blue circles are standard deviations. As shown in Fig. 3, foF2 increases almost linearly with F10.7 values lower than about 180 SFU. However, foF2 apparently shows a saturation effect for F10.7 values higher than about 180 SFU. Such a saturation effect of the ionosphere at higher values of F10.7 and/or sunspot number has also been reported by previous studies [2]-[4]. Theoretically, we expect that the local noon foF2 values would show a good linear relationship with F10.7, because the ionized F-region electron density (foF2) is primarily produced by solar EUV radiation. However, foF2 is saturated for higher F10.7 values. It has been reported that the ionospheric saturation effect for higher F10.7 values is often considerable near the equatorial anomaly region [4]. On the other hand, some previous studies indicate that solar EUV radiation has a nonlinear relationship with F10.7, which is also saturated for higher F10.7 values as seen in foF2 versus F10.7 [3][5]. This result suggests that the F10.7 values at higher solar activity do not quantitatively reflect solar EUV radiation well. In other words, the ionospheric saturation effect results from the nonlinear relationship between F10.7 and solar EUV, and we need to be especially careful when quantitatively discussing the effect of solar activity on ionospheric variation. Section **2.3** gives a detailed description of a better proxy representing solar EUV radiation than F10.7.

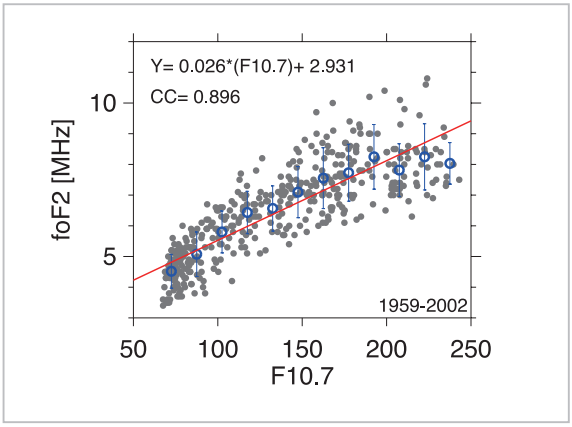

Fig.3 *Monthly median values of foF2 plotted versus monthly mean F10.7 values*

2.2 Seasonal and local time variations

This section describes the seasonal and local time variations in foF2 at Syowa Station, Antarctica. Daily variation in the E-region electron density has a peak around noon, and the electron density lowers toward the nighttime. This is because the E-region electron density at middle and low latitudes is primarily controlled by a balance between the ionization process due to solar radiation and the loss process (recombination). In contrast, daily variation in F2-region electron density is not as simple as that in the E region, but in fact much more complicated. This is because the F2-region electron density is not only affected by the ionization and loss process mentioned above, but also greatly influenced by neutral wind dynamics in the thermosphere. Seasonal variation in F2-region electron density is known to have annual and semiannual variations. In seasonal variation, the neutral composition changes in the thermosphere (particularly the ratio of oxygen atoms to nitrogen molecules ([O]/[N_2])) have implications for the F-region electron density [6]. In addition to the composition and dynamics of the thermosphere (i.e., neutral particles), the precipitation of charged particles and electromagnetic energy from the magnetosphere also play important roles regarding ionospheric variation in the auroral zone (where Syowa Station is located). Moreover, ionospheric variation is also affected by wave activity (tides, gravity waves and planetary waves) propagating from the lower atmosphere [7].

The upper panels in Fig. 4 show the average seasonal and local time dependent variations in foF2 at Syowa Station, Antarctica, for solar minimum (F10.7 < 100, left panel) and for solar maximum (F10.7 > 150, right panel), respectively. White contours are plotted in steps of 0.5 MHz. The black dashed curves represent the respective times at sunrise and sunset. At Syowa Station located in the Southern Hemisphere, the months of November to February correspond to summer, March to April to autumn, May to August to winter, and September to October to spring. Therefore, months on the X-axis are shifted ahead by six months to match the four seasons in the Northern Hemisphere. The middle and lower panels in Fig. 4 show the average seasonal and local time dependent variations in foF2 at Wakkanai in Hokkaido (45.2° N, 141.8° E; 1960 to 2003) and at Kokubunji in Tokyo (35.7° N, 139.5° E; 1959 to 2003), which are located at the middle and low latitudes in

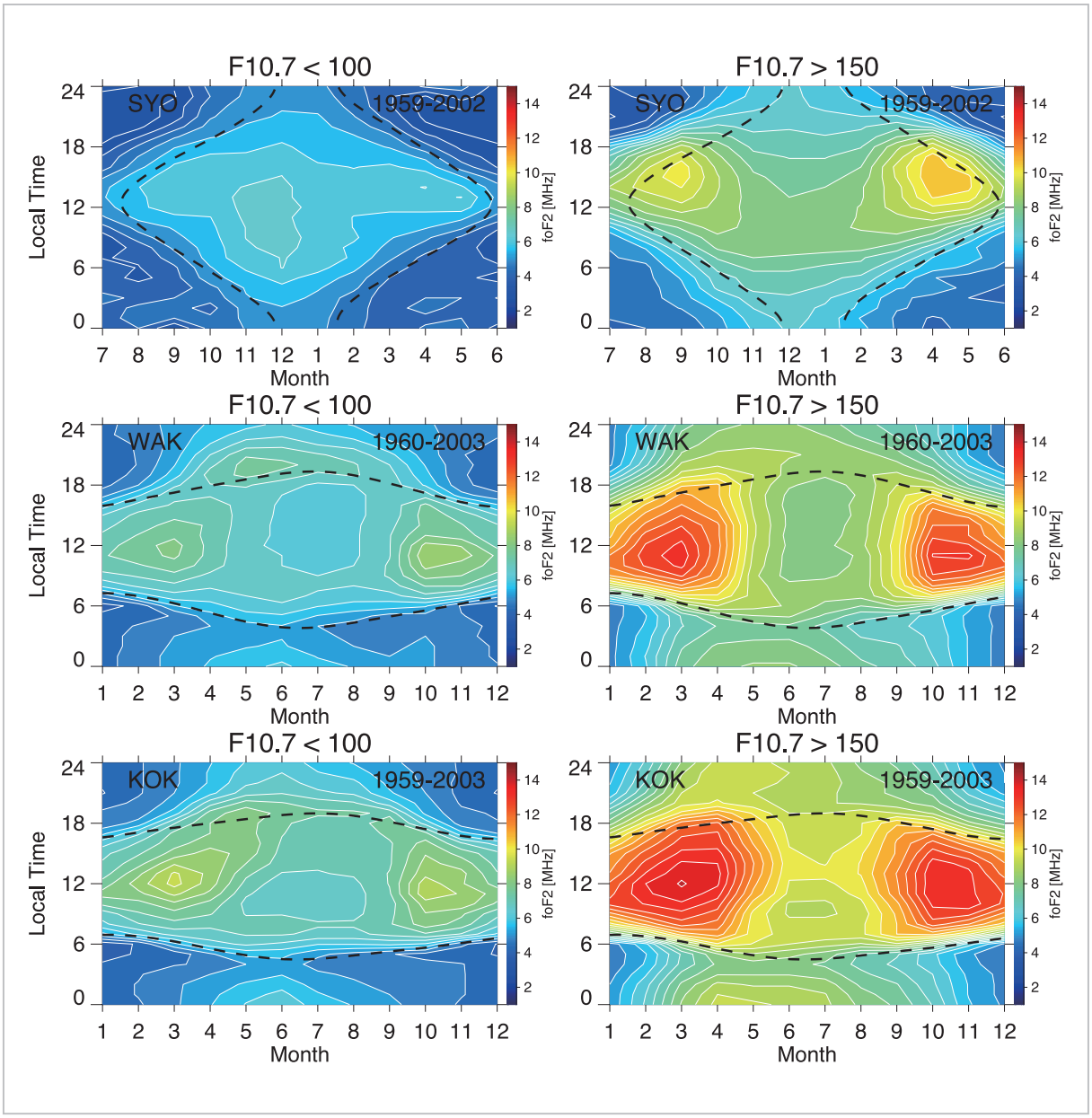

Fig.4 *Average seasonal and local time variations in foF2 during the solar minimum period (F10.7 < 100 in the left figure) and maximum period (F10.7 > 150 in the right figure)*

[Top panels] Syowa Station, Antarctica; [middle panels] Wakkanai; [bottom panels] Kokubunji

Japan, respectively. The major features of foF2 variations seen at Wakkanai and Kokubunji are as follows:

(1) For daytime from 0600 to 1800 LT, semiannual variation with the equinox peaks in spring (March) and autumn (October) exists in foF2 during both the solar maximum and solar minimum. In contrast, for nighttime from 1800 to 0600 LT, annual variation with a peak in summer (May to June) is remarkable.
(2) Both in the solar maximum and solar minimum, foF2 peaks around noon (1200 LT) in autumn, winter and spring, and it tends to become lower toward midnight.
(3) During the summer at Wakkanai, two foF2 peaks appear between 0600 and 0800, and between 1800 and 2000, respectively. At Kokubunji, similar foF2 peaks also appear during the solar minimum period.
(4) During the solar maximum, a considerable foF2 peak around 1200 LT is seen only during summer at Kokubunji, with a structure of multiple peaks formed together with the peak at around midnight.

The seasonal changes and local time changes in foF2 at Syowa Station have both similarities and dissimilarities relative to those at the middle and low latitudes. From Fig. 4, we can see major two differences: first, the foF2 value at Syowa Station is generally about 70% to 80% lower than that at Wakkanai and Kokubunji; secondly, the foF2 variation at Syowa Station shows a quite different tendency during the solar minimum. The main characteristics of seasonal changes and local time changes in foF2 at Syowa Station are as follows:

(1) The foF2 value during the solar minimum shows annual variations, rising in summer and declining in winter.
(2) The daytime foF2 value during the solar maximum shows semiannual variation with peaks in autumn (April) and spring (September).
(3) The daytime foF2 value during the solar maximum is higher in winter than in summer.
(4) The nighttime foF2 value during the solar maximum shows annual variation where it rises in summer and declines in winter.
(5) The peak in the diurnal variation of foF2 changes with the seasons. The peak occurs around 1000 to 1100 LT in summer, 1500 to 1600 LT in spring and autumn, and 1300 to 1400 LT in winter.

The common feature at three observatories is that the daytime foF2 is higher in winter than in summer during the solar maximum. This is presumably due to a rise in the $[O]/[N_2]$ ratio caused by the transport of oxygen atoms from the summer hemisphere to the winter hemisphere [8]. In summer, the oxygen atom density that contributes to ionization decreases, while the density of nitrogen molecules contributing to loss increases. As a result, the $[O]/[N_2]$ ratio in summer decreases considerably. Moreover, the oxygen atoms at F-layer altitudes indicate semiannual variation with peaks in spring and autumn. As solar activity rises, oxygen atom density tends to increase as well. As a result, the daytime foF2 value during the solar maximum presumably shows semiannual variation where it declines in summer, and peaks in spring and autumn. During the solar minimum, however, only Syowa Station shows a different tendency where foF2 is higher in summer than in winter. Considering the sunrise and sunset times indicated in broken lines, we find that the local time and season of the higher foF2 values correspond to the daylight hours. One can consider that the higher foF2 in summer during the solar minimum as seen only at Syowa Station is overwhelmingly more affected by ionization due to longer daylight effects at high latitude, rather than the effects of compo-

sition changes of the neutral atmosphere. This foF2 feature at Syowa Station is quite different from that at middle and low latitudes.

Figure 5 shows the average seasonal changes and local time changes in foE at Syowa Station, Wakkanai, and Kokubunji for reference purposes. However, the data period for foE at Syowa Station is from 1969 to 1979. In general, the foE value corresponds to the peak in the E region electron density. The format of this figure is the same as shown in Fig. 4, except that the contour interval is set to 0.25 MHz. From this figure, one can see that changes in foE at the three observation points are virtually governed by the hours of daylight provided by the sun. However, on the night side of Syowa Station located in the auroral zone, foE rises around spring and autumn. This tendency may be related to geomagnetic activity that peaks in spring and autumn. In other words, enhanced geomagnetic activity leads to more auroral particle precipitation,

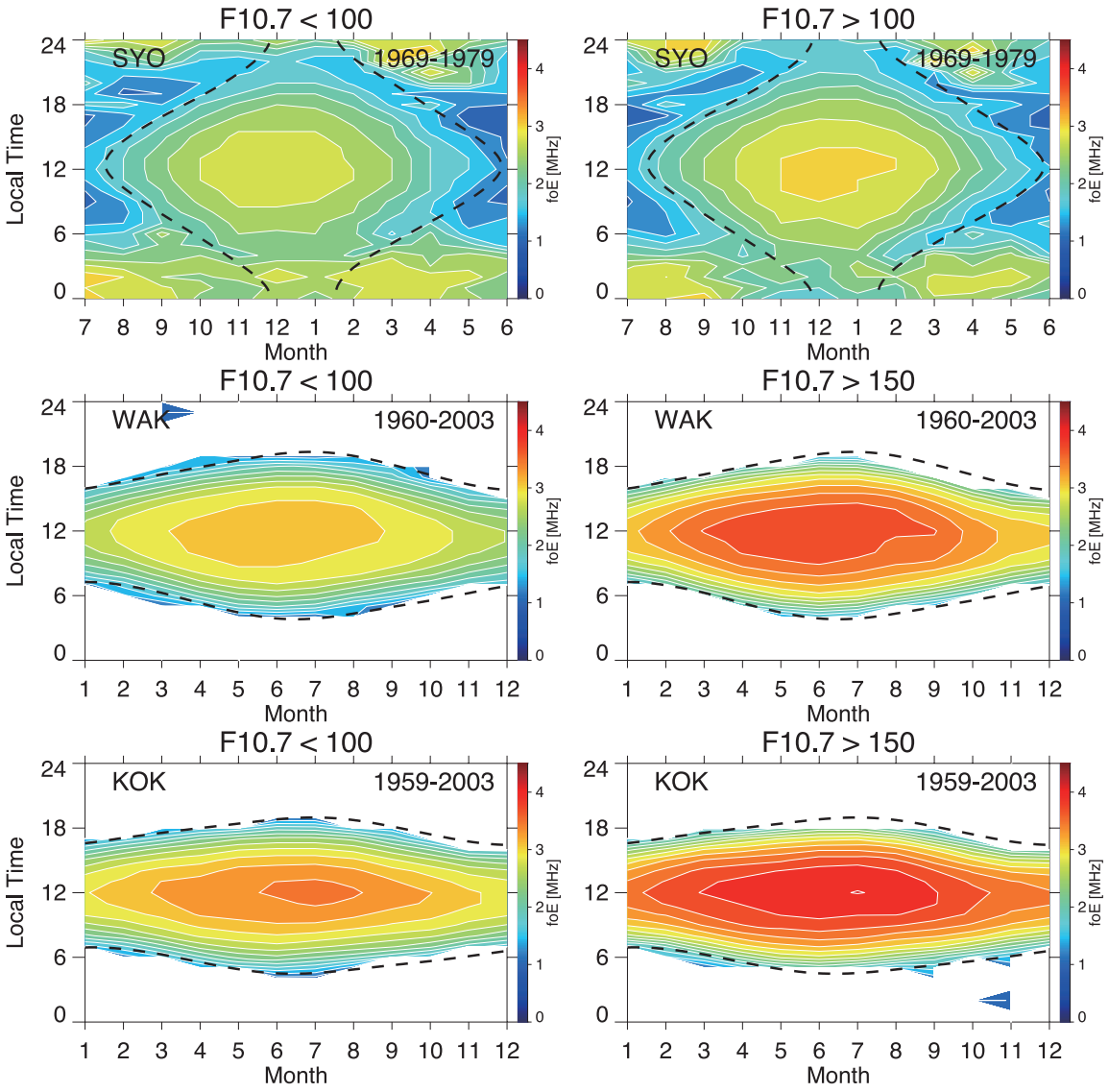

Fig.5 *Average seasonal and local time variations in foE during the solar minimum (F10.7 < 100 in the left figure) and maximum (right figure: F10.7 > 150) at Syowa Station*

[Top panels], Antarctica, Wakkanai [middle panels], and Kokubunji [bottom panels]

thereby ionizing neutral particles in the nightside E region.

2.3 Dependence on solar and geomagnetic activity

As stated in Section **2.1**, foF2 becomes saturated at high levels of F10.7. One presumable cause is that F10.7—a kind of solar activity index—does not completely reproduce the changes in solar EUV radiation that most affects ionospheric generation. Reference [9] compares the four solar activity indexes, sunspot number (SSN), F10.7, MgII (Mg II core-to-wing ratio), and He I (1083) bright line with the solar EUV radiation observed by a satellite. "Sunspot number" means observed portions of the sun that look like black dots or pieces of mass, and is also referred to simply sunspots. These portions actually radiate light as well but appear dark because they emit weaker light than surrounding areas. Sunspots are lower in temperature and also provide stronger magnetic fields than the surrounding areas. MgII is an index that represents the amount of radiation with a wavelength of bright emission lines of magnesium (near 280 nm) in the ultraviolet region [10]. MgII data connect solar UV radiation data observed by different satellites equipped with different types of observation equipment, thereby building up a long-term database spanning more than 30 years, from November 1978 to the present. The He I (1083) bright line has equivalent width for infrared absorption rays (1083 nm) and is determined from solar surface images observed on the ground [11]. He I (1083) is known to reproduce more time series changes in solar UV radiation than F10.7 and SSN [12]. The *SOHO* satellite—a solar observation satellite launched in 1995—is equipped with equipment (solar EUV monitor SEM) for measuring solar EUV radiation, which is considered the most important of all solar radiations contributing to the generation of ionospheric electron density. By comparing the changes in solar EUV radiation observed by SEM with changes in the solar activity indexes of F10.7 and MgII, we have found that MgII is a better indicator of changes in solar EUV radiation than F10.7 [9][13]. Figure 6 is taken from Reference [9] as an example. This figure compares MgII during about four months (from October 1996 to January 1997) with changes in solar EUV radiation, SSN, and F10.7 as observed with SEM. As is evident from this figure, F10.7 and sunspot number have not well reproduced short-term changes and their amplitudes in solar EUV radiation over a period of about 27 days, which is the rotation period of the sun. Conversely, MgII well reproduced the time changes in short-term solar EUV radiation.

MgII is disadvantageous, however, in that its data period is limited to 1978 and later. To compare it with long-term data from the ionosphere available in and after 1959, it is necessary to provide solar activity index data for long periods just like F10.7. Recently, an attempt was made to derive a new solar activity index known as C10.7 (corrected solar flux index) from long-term time series data of F10.7 based on an experience model adopting

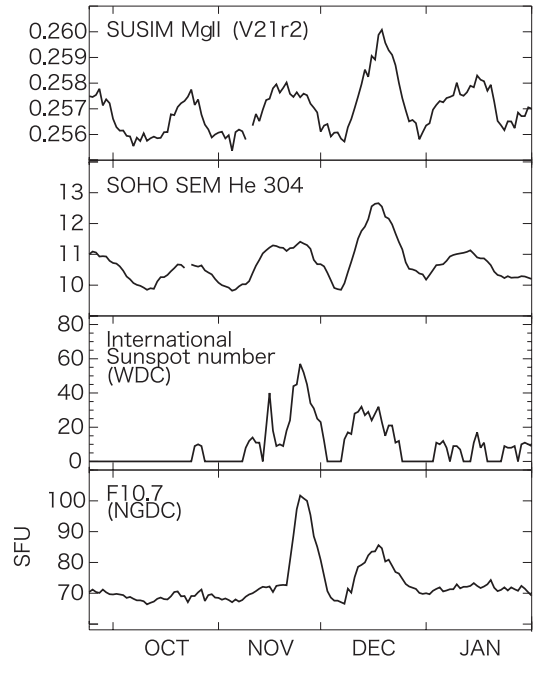

Fig.6 *Comparison of MgII, solar EUV radiation, SSN, and F10.7 during four months from October 1996 to January 1997 (revised version of Fig. 5 of Reference [9])*

a neutral network [14]. C10.7 is an index derived by separating the solar rotation change component of 27 days and the gradual change component from F10.7 based on the statistical nature of F10.7 and solar EUV radiation, for comparison with the changes in solar EUV radiation observed by the SEM of *SOHO*. Still in the development stage, C10.7 is being enhanced to better approximate itself with changes in solar EUV radiation. Here, the first step is to compare the first version of C10.7 with MgII, thereby validating the propriety of C10.7. Figure 7 is a scatter diagram of F10.7 and MgII, and C10.7 and MgII from 1979 to 2002. The correlation with MgII is higher in C10.7 than F10.7 and the square root (RMSE) of average square error—an indicator of the degree of data variance—is also small. Moreover, as F10.7 rises, we can see that MgII becomes saturated. In contrast, C10.7 exhibits no such thing.

The first version of C10.7 or continuous solar activity index data over long periods that better represents changes in solar EUV radiation was therefore used to again investigate the dependence of foF2 on solar activity from 1969 to 2002. In this analysis based on a data set consisting of three data items [foF2 (the average from 1100 to 1300 LT), F10.7, and C10.7], the response differences in daytime foF2 to F10.7 and to C10.7 were examined, respectively. The top and bottom panels in Fig. 8 show scatter diagrams (the gray circle) representing the relation between F10.7 and foF2, and that between C10.7 and foF2. The straight line indicated in each diagram is a linear regression straight line. The correlation factor between F10.7 and foF2 during this data period was 0.686. As shown in Fig. 3, as F10.7 rises, the foF2 value can be seen becoming saturated. Moreover, F10.7 shows large variances in foF2 between 150 and 200 SFU, with many values showing particularly high foF2 (more than 10 MHz). In contrast, the correlation factor between C10.7 and foF2 was 0.716, or a little higher than in the case of

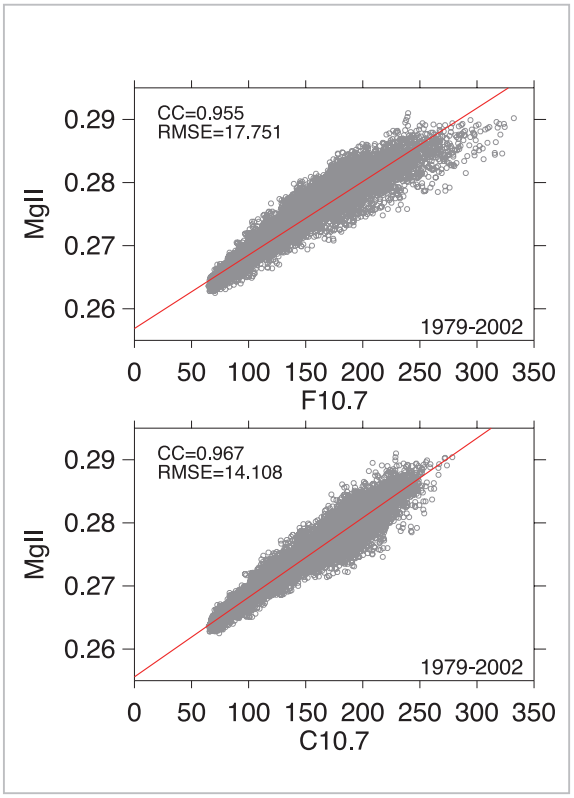

Fig.7 *(Top panel) Comparison of F10.7 and MgII from 1979 to 2002; (bottom panel) comparison of C10.7 and MgII during same period*

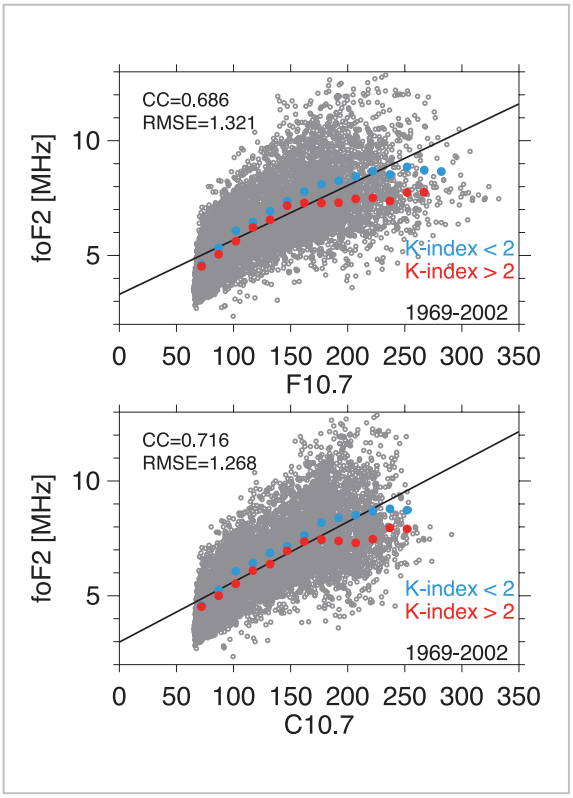

Fig.8 *(Top panel) Comparison of F10.7 and foF2 from 1969 to 2002; (bottom panel) comparison of C10.7 and foF2 during same period*

F10.7. Unlike the case of F10.7, foF2 shows little saturation effect when C10.7 is high, and is generally known to exhibit an almost linear relation. Moreover, RMSE indicates that C10.7 shows smaller variances (error) than F10.7.

Next, we have examined the dependence of geomagnetic activity on foF2. Here, the K-index of Syowa Station is used as an indicator of geomagnetic activity. The K-index indicates geomagnetic activity using numbers from 0 to 9 every three hours based on horizontal magnetic field changes in geomagnetism at each magnetic observation point. For example, the K-index is low during quiet periods of geomagnetic activity, and becomes high during more intense activity. The blue and red circles in the figure denote differences in the dependence of foF2 on solar activity due to geomagnetic activity. The blue circle indicates a quiet activity level (with a K-index of 0 to 2); the red circle indicates a moderate activity level (with a K-index of 2 to 4). Both are used to express the average foF2 when divided for each 15 SFU. In the case of F10.7, foF2 tends to show lower saturation effect at quiet geomagnetism than at geomagnetic disturbance. At 200 SFU or more, however, a slight saturation effect is seen (blue circle in top panel of the figure). Conversely, in the case of C10.7, foF2 shows hardly any saturation effect at quiet geomagnetic activity, thereby suggesting an almost linear relation between C10.7 and foF2 (blue circle in bottom panel of the figure). Even when C10.7 is low (up to 180) at geomagnetic disturbance, it changes almost linearly at the same level as at a quiet level. However, when C10.7 is high (180 or more), foF2 exhibits its saturation effect and becomes lower by about 1 to 2 MHz than at periods of quiet geomagnetic activity. As described above, since C10.7 and solar EUV radiation show almost the same changes, the saturation effect of foF2 seen in the case of C10.7 is presumably due to geomagnetic disturbance. When geomagnetic activity is high (such as auroral activity or a magnetic storm), the electromagnetic energy flowing from the magnetosphere into the polar ionosphere generally increases. At times of such a rising influx of electromagnetic energy, the polar thermosphere will experience changes in atmospheric composition accompanied by higher neutral atmospheric temperature and a lower $[O]/[N_2]$ ratio, thereby reducing the electron density at F layer altitude and resulting in a decline in foF2 (see negative ionospheric storm in Reference [6]). Therefore, in order to maximize the removal of changes in foF2 stemming from geomagnetic disturbance (or an ionospheric storm stemming therefrom) based on long-term time series data on foF2, it is necessary to only select data obtained at periods of quiet geomagnetism (with a K-index of 2 or less). This is related to the method of extracting foF2 long-term trends described in the next section.

3 Long-term trend-relation with global warming

3.1 Review of long-term trend studies

During the late-1980s, a theory was proposed to the effect that an increase in greenhouse gases emitted from the ground surface would warm up the troposphere, while cooling the stratosphere, mesosphere, and thermosphere. Carbon dioxide—a representative greenhouse gas—absorbs and radiates the earth's radiation (infrared rays). Greenhouse gases in the troposphere absorb large quantities of infrared rays radiated by the earth, thereby heating up the atmosphere. In contrast, the middle and upper atmosphere have much lower quantities of infrared rays due to the earth's radiation, so that more radiation is emitted into space than the amount of infrared rays absorbed, thereby resulting in a cooling effect. Moreover, cooling in the stratosphere is not only affected by the direct effects of these greenhouse gases but also by indirect effects due to the decline and loss of ozone caused by chlorine-based compounds. Ozone depletion reduces the heating effect due to the solar ultraviolet absorption of stratospheric ozone. If greenhouse gases continue rising at present

levels, not only will cooling be promoted in the middle and upper atmosphere, but also concerns raised about the various possible changes in the earth's surrounding environment, such as changes in neutral atmospheric density, the denaturing of the atmospheric composition, and the plasma environment. Therefore, it is necessary to clarify what kind of changes occurred in the "field" of the upper atmosphere and ionosphere over a long-term scale of several past decades, and quantitatively understand the effects stemming from natural sources (such as solar and geomagnetic activity) included in long-term change trends and those (such as greenhouse gases) attributed to human sources.

Reference [15] describes the use of a global mean (one-dimensional) atmospheric model, consisting of the mesosphere, thermosphere and ionosphere as a connection system, to quantitatively estimate for the first time the effects of rising greenhouse gases on the atmospheric environment at altitudes of 60 to 500 km. In this numerical simulation, doubling the concentration of greenhouse gases at an altitude of 60 km (as projected to be reached by the end of the 21st century) would result in a predicted drop in temperature by about 10 to 15K at mesospheric altitudes, and about 20 to 50K at thermospheric altitudes. At the same time, atmospheric shrinking occurs with cooling and the density of nitrogen molecules, oxygen molecules and atoms—the main components of the atmosphere in the thermosphere—declines by about 30% to 50%. In connection with changes in the upper atmosphere accompanied by such a rise in greenhouse gases, a decline in ionospheric altitude accompanied by atmospheric shrinking, changes in ionospheric electron density accompanied by changes in the density ratio of oxygen atoms and nitrogen molecules, a rise in methane and water steam density, and more frequent formation of noclilucent clouds accompanied by lower temperature at the mesospheric interface are projected to occur.

Reference [16] describes the use of numerical calculation prediction taken from Reference [15] and standard ionospheric theory to roughly estimate the effects of rising greenhouse gases on the ionosphere. Based on a doubling of the amount of greenhouse gases in the future, it was estimated that the electron density peak altitudes of the ionospheric E layer and F2 layer would drop by about 2 km and 15 to 20 km, respectively. Conversely, hardly any change is seen in electron density not over-sensitively reactive to temperature changes in the neutral atmosphere. The effects on the global ionosphere were then verified by using a three-dimensional thermosphere-ionosphere integration model. Next, similar to the estimates described above, along with the doubling of greenhouse gas concentrations, the peak altitude of the ionospheric F2 layer would drop globally by about 10 to 20 km [17], a finding that began drawing public attention to the effects of greenhouse gases on the ionosphere. If such ionospheric changes do indeed occur in the future, serious concerns will be raised over the effects on radio wave communications and related fields already put to practical use.

The neutral atmospheric density of the thermosphere can be estimated by determining the rate of change in the orbital radius due to atmospheric drag imposed on satellites as based on orbital data obtained from low-altitude satellites orbiting at thermospheric altitudes. Reference [18] clarified that the atmospheric density at altitudes of 300 to 400 km declines by about 0.45% per year on average based on satellite orbits during the three previous minimal periods (in 1976, 1986 and 1996) of solar activity. If the thermospheric atmospheric density declines linearly at this rate of decline, the end of the 21st century will see a drop in the thermosphere by as much as about 40 km due to cooling. This high decline in thermospheric density receives hardly any influence from geomagnetic activity, local time and season, but does tend to depend on altitude and solar activity. For example, the decline in atmospheric density tends to be greater at higher altitudes, and the decline in atmospheric density tends to be higher during

a minimal period rather than a maximum period of solar activity[19]. These trends agree well in qualitative terms with the results estimated based on the model described in Reference[17], though the magnitude of the decline in density estimated from observations is a little greater than reported in the model results. Since the model study presented in Reference[17], higher activity has been seen in studies attempting to detect long-term ionospheric trends based on ground-based observational data. The method of multiple regression analysis is often used in many cases when long-term trends of the ionosphere are detected. Multiple regression analysis is a method of examining the relation between dependent variables and one or more independent descriptive variables considered to affect those variables, in order to determine their interrelational equation (multiple regression equation). Reference[20] reported observation results that for the first time support a decline in ionospheric altitude caused by cooling of the super-high layer atmosphere as predicted from model calculations. Reference[20] used long-term (1957–1990) data observed with an ionosonde at medium altitudes since IGY in order to clarify that the peak altitude of the ionospheric F2 layer has shown a gradual downward trend over the past three decades. Moreover, the annual decline in peak altitude of this ionospheric F2 layer turned out to be more considerable in winter (−0.45 km/yr) than in summer (−0.12 km/yr). Ionosonde data observed in and after 1958, in Northern Europe at Sodankyla, Finland (latitude 67° north, longitude 27° east), was then used to again report that the peak altitude of the ionospheric F2 layer has been falling over long periods[21][22].

Reference[23] used long-term ionosonde data taken at Tromsø, Norway (latitude 69° north, longitude 19° east) from 1935 to 2001 to demonstrate a long-term downward trend in foF2 (−0.0078 MHz/yr). Reference[23] considered that this downward trend in foF2 was due to a rise in greenhouse gases, as well as changes in oxygen atoms and nitrogen molecules. Reference[24] used data obtained from an observation network of multiple ionosondes located in the Northern Hemisphere to investigate altitude changes in long-term trends in foF2. While the long-term trends in foF2 show a downward trend at most observation points, another trend showed that the rate of decline in long-term trends in foF2 rises as altitude increases. This dependence of these long-term trends in foF2 on altitude is interpreted to mean the effects of ionospheric storms due to geomagnetic activity.

Analysis conducted with a multi-point observation network of ionosondes installed in various parts of the world, however, reports that long-term trends at the peak altitude of the F2 layer do not reflect globally monotonous negative trends, although some positive trends are seen at certain observation points[25]–[27]. Reference[27] shows the world distribution of trends in F2 layer peak altitude and points out that, although the growth trends of F2 layer peak altitudes are not dependent on latitude or longitude, these trends do reflect a certain degree of regionality. The mechanism to describe this regionality, however, has yet to be understood. Such a complex trend distribution contradicts the numerical model results given in References[15][17] that predict cooling of the global super-high layer atmosphere due to rising greenhouse gases. For that reason, some studies have even reported that long-term trends in F2 layer peak altitudes are not due to cooling of the upper atmosphere caused by rising greenhouse gases, but due to long-term changes in geomagnetic activity[24][28].

The reality is that no uniform view has yet been obtained about the long-term trends of the ionospheric F2 layer as determined using ionosondes, unlike the long-term trends of global thermospheric atmospheric density based on satellite orbital data.

3.2 Long-term ionospheric trends observed at Syowa Station

The previous studies described above attempted to estimate long-term ionospheric

trends by using various methods. The most important thing in estimating long-term ionospheric trends is finding a way to remove a component that depends on solar and geomagnetic activity from the variable components of the ionosphere. The effects of geomagnetic activity are particularly pronounced at Syowa Station, which is located in the auroral zone. What is common to most of the previous long-term trend studies is that a linear relation is assumed between foF2 and the solar activity indexes (SSN and F10.7) when expressing the changes in foF2 stemming from solar activity. However, as shown in Figs. 3 and 8, when F10.7 is high, foF2 becomes higher in terms of saturation effect, resulting in a degraded linear relation. For that reason, when using SSN and F10.7, one cannot well express changes in foF2 dependent on solar activity. And as described in Section **2.3**, foF2 becomes higher in saturation effect along with rising geomagnetic activity (see Fig. 8). This analysis therefore used C10.7—an index that better reproduces changes in solar EUV radiation—as a solar activity index. Only those items of data obtained during quiet periods of geomagnetic activity ($0 \leqq$ K-index $\leqq 2$) from 1100 to 1300 at the local time each day were used for foF2, thereby minimizing the effect of geomagnetic disturbance. It is known that ionospheric disturbance generally continues with a certain time constant even after a geomagnetic disturbance. However, its effect is ignored here. From these two conditions, the long-term trends in foF2 from 1969 to 2002 (where the K-index can be used) were first derived. The following gives a detailed description of the method used for derivation:

(1) From the foF2 data observed ($foF2_{obs}$), select only the data obtained during quiet periods of geomagnetic activity ($0 \leqq$ K-index $\leqq 2$).

(2) Assume a linear relation between C10.7 and foF2, and determine the component that changes depending only on solar activity ($foF2_{mod} = a_I \bullet C10.7 + b_I$) from foF2 observed.

(3) Subtract $foF2_{mod}$ from the observed $foF2_{obs}$ to obtain the residual error component ($\Delta foF2 = foF2_{obs} - foF2_{mod}$) as a change independent of solar and geomagnetic activity.

(4) Determine the linear regression equation [$\Delta foF2 = A + B^* (year - 1969)$] and regard its inclination B as the long-term trend of foF2.

Figure 9 (a) shows the change ($foF2_{obs}$: gray circle) in foF2 observed from 1969 to 2002 and the component ($foF2_{mod}$: blue line) of foF2 dependent on solar activity as obtained by using F10.7. Moreover, Fig. 9 (b) shows the residual error in foF2 ($\Delta foF2$: gray circle) and the linear trend obtained therefrom (blue line). In contrast, Fig. 9 (c) and (d) show the component ($foF2_{mod}$: red line) of foF2 that depends on solar activity when using C10.7 and the linear trend obtained therefrom (red line). The linear trend of foF2 from 1969 to 2002 showed a tendency where a decline occurs by -0.0002 ± 0.0018 MHz per year when using F10.7. However, in that case, since the trend component is smaller than the error, the long-term trend component can be regarded as almost zero. Conversely, when C10.7 is used, the long-term trend of foF2 declined by -0.0012 ± 0.0017 MHz per year, thereby marking an approximate sixfold increase in the rate of decline (inclination) as compared with F10.7. From this result, one can also see that long-term trends vary according to the solar activity index selected. This suggests that previous analysis methods need to be reconsidered. In the case of C10.7 as well, since the trend component is slightly smaller than the error, one cannot necessarily assert that foF2 showed a significantly downward trend from 1969 to 2002. Although this is a different method, it yields a different result than that described in Reference [23] where a trend showing a significant decline in foF2 (annual decline of -0.0078 ± 0.0041 MHz) was derived from foF2 long-term data obtained at Tromsø from 1935 to 2001.

Next, the author examined how much the long-term trends of foF2 derived are affected by different methods of extracting trends, the

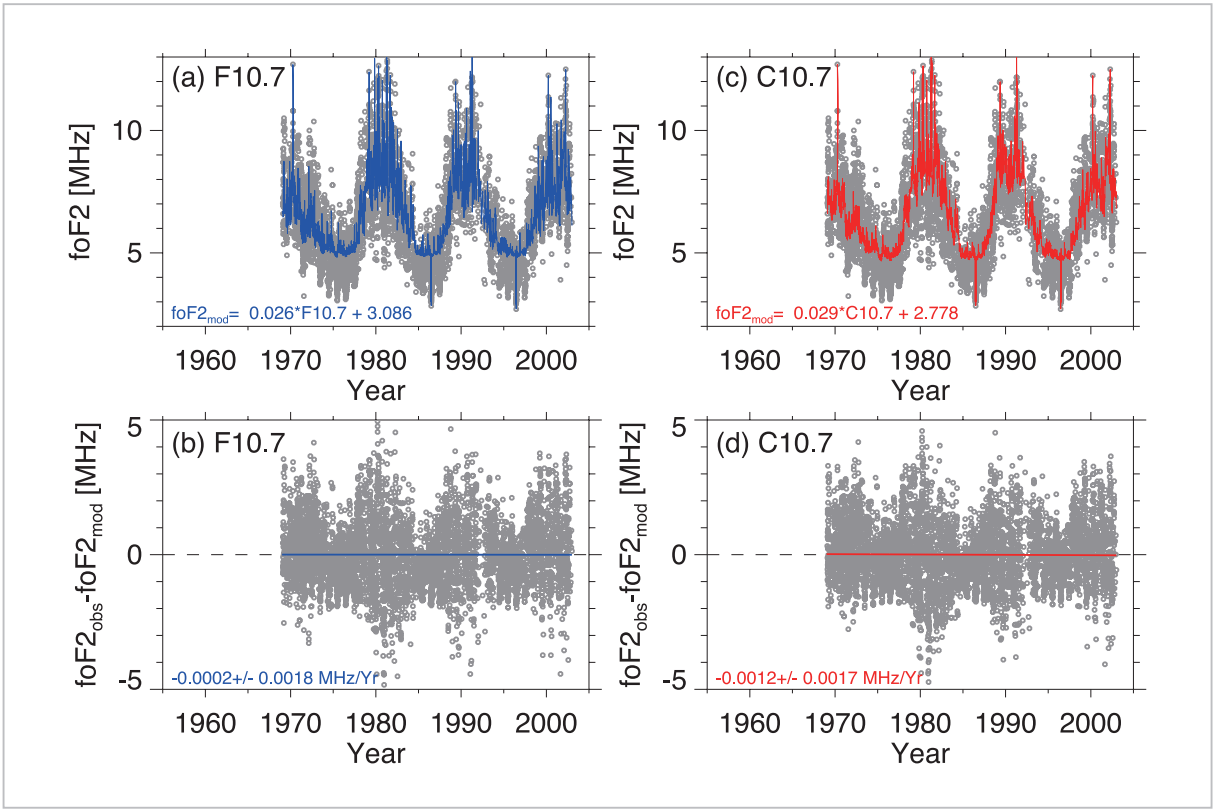

Fig.9 *(a) Changes (foF2abs: gray circle) in foF2 observed from 1969 to 2002 and the foF2 component (foF2mod: blue line) dependent on solar activity as obtained by using F10.7 (b) Residual component of foF2 (ΔfoF2: gray circle) and linear trend (blue line) (c) Changes in foF2 observed from 1969 to 2002 (foF2obs: gray circle) and the foF2 component (foF2mod: red line) dependent on solar activity as observed by using C10.7 (d) Residual component of foF2 (ΔfoF2: gray circle) and linear trend (red line)*

data period, and solar activity indexes used. Solar activity indexes (F10.7 and C10.7) and geomagnetic activity indexes (K-index and ap index) were used as the data. The ap index is a value measured every three hours to represent the activity of geomagnetism based on observations taken at geomagnetic observatories in 12 countries around the world, and is divided into 28 sections between 0 and 400 nT. In this analysis, quiet geomagnetism was defined as a level where the ap index was 10 nT or less. Table 1 summarizes the long-term trend values of foF2. Three cases were considered for the model value of foF2 ($foF2_{mod}$). In model 1, the component dependent on solar and geomagnetic activity was expressed as $foF2_{mod} = a_1$.(solar activity index) + b_1.(geomagnetic activity index: ap index) + c_1; the trend component was determined by subtracting both indexes from the observation values. This is one of the methods used in previous long-term trend studies of the ionosphere. Models 2 and 3 were judged by using the ap index (of 10 or less) and K-index (of 2 or less), respectively, in order to extract only the foF2 at quiet geomagnetic activity. The method used for that purpose was the same method as indicated at the beginning. As can be seen from Table 1, regardless of the method used, the long-term trend component of foF2 shows a downward trend, but the rate of decline in that trend varies greatly in line with differences in the observation data period, solar activity index, and method of trend extraction. The method using model 2 showed the greatest downward trend, followed by the method in model 1. According to the method in model 3, the long-term trend in foF2 is almost zero. The long-term trends from 1959 to 2002 showed no such major differences due to differences in the solar activity index, but those differences become much more pronounced when divided

Table 1 *Long-term trends in foF2 at Syowa Station derived from differences in method of trend extraction, data period, and solar activity index*

	Solar activity index (S)	$foF2_{mod} = a \cdot S + b \cdot ap + c$	$foF2_{mod} = a \cdot S + b$ ap index ≤ 10	$foF2_{mod} = a \cdot S + b$ K index ≤ 2
1959–2002	F10.7	**–0.0033±0.0013 MHz/Yr**	**–0.0066±0.0016 MHz/Yr**	
	C10.7	**–0.0028±0.0013 MHz/Yr**	**–0.0063±0.0015 MHz/Yr**	
1969–2002	F10.7	**–0.0016±0.0016 MHz/Yr**	**–0.0040±0.0018 MHz/Yr**	**–0.0002±0.0018 MHz/Yr**
	C10.7	**–0.0033±0.0015 MHz/Yr**	**–0.0053±0.0017 MHz/Yr**	**–0.0012±0.0017 MHz/Yr**
1979–2002	F10.7	**+0.0154±0.0028 MHz/Yr**	**+0.0135±0.0033 MHz/Yr**	**+0.0152±0.0044 MHz/Yr**
	C10.7	**+0.0190±0.0027 MHz/Yr**	**+0.0171±0.0032 MHz/Yr**	**+0.0213±0.0042 MHz/Yr**
	MgII	**+0.0147±0.0030 MHz/Yr**	**+0.0104±0.0035 MHz/Yr**	**+0.0222±0.0042 MHz/Yr**

by the data periods from 1969 to 2002.

The findings above provide important tips on proceeding with long-term trend analyses in the future. In deriving global long-term trends of the ionosphere, it is vital to conduct revalidation after establishing: (1) an alignment of data observation periods at respective observation points, (2) a method of removing the component dependent on solar and geomagnetic activity, and (3) selecting solar and geomagnetic activity indexes, and related factors.

4 Conclusion

The ionosphere is a region that exercises an important influence on communications and radio wave propagation. It is affected by both top and bottom, and its daily changes, seasonal changes, and other changes behave in a complex manner. In recent years, some researchers have pointed out the possibility that a rise in greenhouse gases attributed to human activity may be playing an important role in changes occurring in the earth's super-high layer atmosphere (ionosphere) over a long time scale. As such, the ionosphere is very important as a boundary region in the top-bottom connection of the earth's atmosphere.

This paper introduced various changes in the ionospheric F2 layer in the auroral zone based on long-term observation data taken from 1959 to 2002 using an ionosonde at Syowa Station, Antarctica (69.0° S, 39.6° E). The average local time and seasonal changes in foF2 show complex changes that can also be seen at other observation points, and were found to greatly affect solar and geomagnetic activity. Moreover, the long-term trends in the ionosphere considered to affect global warming are issues of great concern in social as well as scientific terms. In the future, it will be necessary to continue ionospheric observations at Syowa Station and clarify ionospheric changes over an even longer time scale, while taking an approach based on a numerical model in order to understand the physical processes behind those changes.

Acknowledgments

The National Geophysical Data Center (NGDC), NOAA, provided the F10.7 index and MgII. Mamoru Ishii, director of the Applied Electromagnetic Research Center, National Institute of Information and Communications Technology (NICT), and Maho Nakamura, chief researcher, Light and Space-Time Standards Group, also of NICT, provided the ionosonde data obtained from Syowa Station in Antarctica. The author also wishes to express profound thanks to senior researcher Takaue Maruyama and chief

researcher Maho Nakamura of NICT for the valuable advice they provided. The author also thanks Ms. Fukushima of NICT for having taken the readings of ionogram data from Syowa Station for many long years. Last but not least, the author thanks all the Antarctic observation team members engaged in installing and maintaining the ionosonde observation equipment at Syowa Station.

References

1 Rishbeth, H., "The centenary of solar-terrestrial physics," J. Atmos. Solar Terr. Phys., 63, 1883–1890, 2001.
2 Lakshmi, D. R., B. M. Reddy, and R. S. Dabas, "On the possible use of recent EUV data for ionospheric predictions," J. Atmos. Terr. Phys., 50, 207–213, 1988.
3 Balan, N., G. J. Bailey, B. Jenkins, P. B. Rao, and R. J. Moffett, "Variations of Ionospheric Ionization and Related Solar Fluxes During an Intense Solar Cycle," J. Geophys. Res., 99(A2), 2243–2253, 1994.
4 Liu, J. Y., Y. I. Chen, and J. S. Lin, "Statistical investigation of the saturation effect in the ionospheric foF2 versus sunspot, solar radio noise, and solar EUV radiation," J. Geophys. Res., 108(A2), 1067, doi: 10.1029/2001JA007543, 2003.
5 Richards, P. G., J. A. Fennelly, and D. G. Torr, "EUVAC: A Solar EUV Flux Model for Aeronomic Calculations," J. Geophys. Res., 99(A5), 8981–8992, 1994.
6 Rishbeth, H., "How the thermospheric composition affects the ionospheric F2-layer," J. Atmos. Solar Terr. Phys., 60, 1385–1402, 1998.
7 Rishbeth, H. and M. Mendillo, "Patterns of F2-layer variability," J. Atmos. Solar Terr. Phys., 63, 1661–1680, 2001.
8 Torr, M. R. and D. G. Torr, "The seasonal behaviour of the F2-layer of the ionosphere," J. Atmos. Terr. Phys., 35, 2237–2251,1973.
9 Floyd, L., J. Newmark, J. Cook, L. Herring, and D. McMullin, "Solar EUV and UV spectral irradiances and solar indices," J. Atmos. Solar Terr. Phys., 67, 3–15, 2005.
10 Heath, D. F., and B. M. Schlesinger, "The Mg 280 nm doublet as a monitor of changes in the solar ultraviolet irradiance," J. Geophys. Res., 91, 8672–8682, 1986.
11 Harvey, J. W. and W. C. Livingston, "Variability of the solar He I 10830 angstrom triplet, IAU Symposium 154, Infrared Solar Physics," 59, 1994.
12 Donnelly, R. F., T. P. Repoff, J. W. Harvey, and D. F. Heath, "Temporal characteristics of the solar UV flux and He I line at 1083 nm," J. Geophys. Res., 90, 6267–6273, 1985.
13 Viereck, R., L. Puga, D. McMullin, D. Judge, M. Weber, and W. K. Tobiska, "The Mg II index: A proxy for solar EUV," Geophys. Res. Lett., 28(7), 1343–1346, 2001.
14 Maruyama T., "Regional Reference Total Electron Content Model over Japan Using Solar EUV Proxies," Special issue of this NICT Journal, 3–3–5, 2009.
15 Roble, R. G. and R. E. Dickinson, "How will changes in carbon dioxide and methane modify the mean structure of the mesosphere and thermosphere ?," Geophys. Res. Lett., 16, 1441–1444, 1989.
16 Rishbeth, H., "A greenhouse effect in the ionosphere ?," Planet. Space Sci., 38, 945–948, 1990.
17 Rishbeth, H. and R. G. Roble, "Cooling of the upper atmosphere by enhanced greenhouse gases -Modeling of thermospheric and ionospheric effects," Planet. Space Sci., 40, 1011–1026, 1992.
18 Keating, G. M., R. H. Tolson, and M. S. Bradford, "Evidence of long term global decline in the Earth's thermospheric densities apparently related to anthropogenic effects," Geophys. Res. Lett., 27(10), 1523–1526, 2000.

19 Emmert, J. T., J. M. Picone, J. L. Lean, and S. H. Knowles, "Global change in the termosphere: Compelling evidence of a secular decrease in density," J. Geophys. Res., 109, A02301, doi: 10.1029/2003JA010176, 2004.
20 Bremer, J., "Ionospheric trends in mid-latitudes as a possible indicator of the atmospheric greenhouse effect," J. Atmos. Terr., Phys., 54, 1505–1511, 1992.
21 Ulich, T. and E. Turunen, "Evidence for long-term cooling of the upper atmosphere in ionosonde data," Geophys. Res. Lett., 24, 1103–1106, 1997.
22 Ulich, T., M. Cliverd, and H. Rishbeth, "Determining long-term change in the ionosphere," EOS, 84, 581, 2003.
23 Hall, C. M. and P. S. Cannon, "Trends in foF2 above Tromsø(69°N 19°E)," Geophys. Res. Lett., 29, 2128, doi: 10.1029/2002GL016259, 2002.
24 Mikhailov, A. V. and D. Marin, "Geomagnetic control of the foF2 long-term trends," Ann. Geophys., 18, 653–665, 2000.
25 Bremer, J., "Trends in the ionospheric E and F regions over Europe," Ann. Geophys., 16, 986-996, 1998.
26 Upadhyay, H. O. and K. K. Mahajan, "Atmospheric greenhouse effect and ionospheric trends," Geophys. Res. Lett., 25, 3375-3378, 1998.
27 Bremer, J., "Investigations of long-term trends in the ionosphere with world-wide ionosonde Observations," Adv. Radio Sci., 2, 253–258, 2004.
28 Mikhailov, A. V., and D. Marin, "An interpretation of the foF2 and hmF2 long-term trends in the framework of the geomagnetic control concept," Ann. Geophys., 19, 733–748, 2001.

***MOTOBA Tetsuo**, Dr. Sci.*
Project Researcher, Space and Upper Atmospheric Sciences Group, National Institute of Polar Research
Upper Atmospheric Physics